Molecular Pharmacology Fast Forward. Published on February 26, 2007 as doi:10.1124/mol.106.033092
This article has not been copyedited and formatted. The final version may differ from this version.

Agonist-driven conformational changes in the inner β-sheet of α7 nicotinic receptors

James T. McLaughlin, Jie Fu, and Robert L. Rosenberg

Departments of Pharmacology (JTM, JF, and RLR) and Cell & Molecular Physiology (RLR), University of North Carolina at Chapel Hill, Chapel Hill, NC 27599-7365

Molecular Pharmacology Fast Forward. Published on February 26, 2007 as DOI: 10.1124/mol.106.033092
This article has not been copyedited and formatted. The final version may differ from this version.

Running Title: Agonist-driven changes in the inner β-sheet of α7 AChRs

Corresponding Author: Dr. Robert L. Rosenberg

Department of Pharmacology, CB# 7365

University of North Carolina at Chapel Hill

Chapel Hill, NC 27599-7365

Phone: (919) 966-6375 Fax: (919) 966-5640

Email: robert_rosenberg@med.unc.edu

Number of text pages: 27

Number of Figures: 6

Number of Tables: 1

Number of References: 33

Number of words in Abstract: 250

Number of words in Introduction: 736

Number of words in Discussion: 1569

Non-standard ABBREVIATIONS

AChBP	acetylcholine binding-protein
AChR	nicotinic acetylcholine receptor
ESLC	extracellular recording solution containing low Ca^{2+} concentration
LBD	ligand-binding domain
MTSEA	2-aminoethylmethane thiosulfonate
ND96	*Xenopus* oocyte storage buffer
SCAM	Substituted-cysteine accessibility method
TMD	trans-membrane ion channel domain

Molecular Pharmacology Fast Forward. Published on February 26, 2007 as DOI: 10.1124/mol.106.033092
This article has not been copyedited and formatted. The final version may differ from this version.

Abstract

Cys-loop ligand-gated ion channels assemble as pentameric proteins with each monomer contributing two structural elements: an extracellular ligand-binding domain (LBD) and a transmembrane ion channel domain (TMD). Models of receptor activation include rotational movements of subunits leading to opening of the ion channel. We tested this idea using substituted cysteine accessibility to track conformational changes in the inner β sheet of the LBD. Using a non-desensitizing chick α7 background ($L^{247}T$), we constructed 18 consecutive cysteine replacement mutants (L^{36} to I^{53}) and tested each for expression of ACh-evoked currents and functional sensitivity to thiol modification. We measured rates of modification in the presence and absence of ACh to identify conformational changes associated with receptor activation. Resting modification rates of eight substituted cysteines in the β1 and β2 strands and the sequence between them (loop 2) varied over several orders of magnitude, suggesting substantial differences in the accessibility or electrostatic environment of individual side chains. These differences were in general agreement with structural models of the LBD. Eight of eighteen cysteine replacements displayed ACh-dependent changes in modification rates, indicating a change in the accessibility or electrostatic environment of the introduced cysteine during activation. Surprisingly, we found the effects of agonist exposure were difficult to reconcile with rotational models of activation. Acetylcholine reduced the modification rate of $M^{40}C$ but increased it at $N^{52}C$ despite the close physical proximity of these residues. Our results suggest that models that depend strictly on rigid-body rotation of the LBD may provide an incomplete description of receptor activation.

Molecular Pharmacology Fast Forward. Published on February 26, 2007 as DOI: 10.1124/mol.106.033092
This article has not been copyedited and formatted. The final version may differ from this version.

Introduction

Nicotinic acetylcholine receptors are members of the Cys-loop gene family, a group that also includes $GABA_A$, glycine, and $5\text{-}HT_3$ ionotropic receptors. Cys-loop receptors convert the energy of ligand binding into conformational changes that lead to the opening of transmembrane ion channels (Karlin, 2002). The genes in this family encode bifunctional polypeptides that include both an extracellular ligand binding domain (LBD) and a transmembrane ion channel domain (TMD). These receptors also share a similar quaternary structure of homologous or identical polypeptides assembled as a pentamer around a central pore.

The two major structural elements of these receptors are the ligand binding site and the ion channel. The ligand binding site is located at the interface between two receptor subunits ~30 Å from the membrane. It is formed by a set of conserved aromatic residues positioned "beneath" a flexible loop (the C loop) containing ~15 amino acids (Sine, 2002). The central pore of the receptor contains both the ion permeation pathway and the "gate" that controls ion flow. This pore is lined by the second transmembrane helix (M2) from each subunit (Karlin, 2002). The coupling of agonist binding to the opening of the transmembrane ion channel must involve conformational linkage between these two domains. The functional and sequence homology between members of the family suggests that there may also be a common mechanism underlying the linkage between ligand binding and channel gating (Sine and Engel 2006; Xiu et al., 2005).

Knowledge of the atomic-scale structure of Cys-loop receptors was first obtained from cryo-electron microscopy of AChR from *Torpedo* electric organ (Unwin, 1993).

Molecular Pharmacology Fast Forward. Published on February 26, 2007 as DOI: 10.1124/mol.106.033092
This article has not been copyedited and formatted. The final version may differ from this version.

More recently the X-ray crystal structures of several invertebrate ACh binding proteins (AChBPs) have provided a structural basis for a wealth of biochemical and mutagenesis data (Brejc et al., 2001). The AChBPs exhibit sequence homology to the Cys-Loop LBD, and co-crystals formed with nicotinic agonists or antagonists have confirmed their value in modeling receptor structure based upon a functional homology (Celie et al., 2004; Hansen et al., 2005). Although the AChBPs lack a TMD, Unwin and colleagues used the high resolution of the AChBP X-ray data to refine their models of the *Torpedo* AChR (Unwin et al., 2002; Miyazawa et al., 2003; Unwin, 2005). Using refined cryo-images of AChRs they propose a gating mechanism in which agonist binding leads to rotation of the LBD, particularly in the area of the inner β sheets. They suggest that this rotation is coupled to movements of the M2 transmembrane helix and opening of the ion channel.

Coupling of conformational changes in the LBD to those in the TMD is likely to involve segments positioned at the interface between the LBD domain and the TMD, including loop 2, loop 7, loop 9, pre-M1, and the M2-M3 linker segment (Bouzat et al., 2004; Chakrapani et al., 2004). Salt bridges and salt-bridge switches may be involved in several steps in the activation process (Mukhtasimova et al., 2005; Lee and Sine 2005). There are conformational linkages between loop 2 and the M2-M3 linker in α7 AChRs (Sala et al., 2005) or between loop 2, loop 7 and the M2-M3 linker in $GABA_A$ receptors (Kash et al., 2003). Cis-trans isomerization of a proline in the M2-M3 linker of 5-HT3 receptors provides addition evidence that this segment is a crucial gating element (Lummis et al., 2005). However, many of the specific residues implicated in these studies are not conserved throughout the Cys-loop family, suggesting that there may

Molecular Pharmacology Fast Forward. Published on February 26, 2007 as DOI: 10.1124/mol.106.033092
This article has not been copyedited and formatted. The final version may differ from this version.

not be one universal activation mechanism. A consensus gating mechanism has yet to emerge.

Is subunit rotation required for receptor activation? Previously, we used the substituted-cysteine accessibility method (SCAM; Karlin and Akabas, 1998) to examine agonist-driven movements in α7 AChRs in loop 9 and obtained results that were consistent with an agonist-induced asymmetric rotation of the LBD (Lyford et al., 2003). In this report we use the same approach to examine conformational changes in the inner β sheet of the LBD, focusing on loop 2 and surrounding residues in the β1 and β2 strands (L^{36} to I^{53}). Based upon current models, loop 2 extends into the subunit-subunit interface from the principal binding subunit (+), whereas the β1 and β2 segments line the lower interface of the complementary subunit (-). Using SCAM, we find that side-chain modification rates are generally consistent with the predictions of the structural models. We also find, however, that agonist-dependent changes of modification rates are not consistent with simple rigid-body rotational models of receptor activation.

Molecular Pharmacology Fast Forward. Published on February 26, 2007 as DOI: 10.1124/mol.106.033092
This article has not been copyedited and formatted. The final version may differ from this version.

Materials and Methods

Reagents MTSEA (2-aminoethylmethane thiosulfonate) was obtained from Toronto Research Chemical (Toronto, Canada). Gentamicin was from Invitrogen (Carlsbad, CA). All other reagents were obtained from Sigma-Aldrich (St. Louis, MO).

Site-directed mutagenesis A cDNA clone of the chick α7 receptor containing two mutations ($C^{115}A$, $L^{247}T$) was used as the parental phenotype for mutations described in this study. We mutated the lone unpaired cysteine in the extracellular domain (C^{115}) to allow more straightforward interpretation of MTSEA exposure experiments. We observed no functional effect of this mutation on receptor expression or ACh response. We included the mutation of leucine 247 in the M2 transmembrane domain ($L^{247}T$; L9'T) because of its large current amplitudes and non-desensitizing kinetics compared to wild type α7 receptors (Revah et al., 1991). Mutation at the L9' position enhances our ability to measure modification kinetics for cysteine replacements in which the ACh-evoked current amplitudes are attenuated (Beene et al., 2002). All mutations were introduced by site-directed mutagenesis using the QuickChange method (Stratagene) as described previously (Eddins et al., 2002), and were confirmed by DNA sequencing.

***Xenopus* oocyte maintenance and expression** Oocytes were surgically removed and prepared from female *Xenopus laevis* in accordance with UNC Institutional Animal Care and Use Committee guidelines. cRNA was prepared using the T7 RNA polymerase and mMessage mMachine kit as described by the manufacturer (Ambion/Applied Biosystems, Austin, TX). Oocytes were injected with 20 ng of cRNA and incubated at 18^{o}C in ND96 (96 mM NaCl, 2 mM KCl, 1 mM $MgCl_2$, 1.8 mM $CaCl_2$, 5 mM HEPES pH 7.5) for 2-5 days before use.

Molecular Pharmacology Fast Forward. Published on February 26, 2007 as DOI: 10.1124/mol.106.033092
This article has not been copyedited and formatted. The final version may differ from this version.

Data collection and analysis Oocytes were superfused in normal extracellular solution containing a reduced Ca^{2+} concentration (ESLC; 96 mM NaCl, 2 mM KCl, 1 mM $MgCl_2$, 0.1 mM $CaCl_2$, and 10 mM HEPES, pH 7.5). This solution minimized Ca^{2+} influx and eliminated Ca^{2+}-activated chloride currents. Two-electrode voltage clamp was performed with a GeneClamp 500B controlled by pCLAMP6 software (Axon Instruments). Electrodes were filled with 3 M KCl contacting Ag-AgCl wires and had resistances of 0.5 to 2.0 MΩ. Currents were recorded at a constant holding potential of -60 mV. Currents were low pass filtered at 50 Hz and sampled at 100 Hz. Agonist dose-response curves were obtained as described previously (Eddins et al., 2002), and data were fit to the Hill equation using Origin software.

Expression and modification kinetics Each mutant was initially screened for functional expression over a range of ACh concentrations to generate a dose-response relationship and determine its EC_{50}. To test for reactivity of introduced free thiols, we compared responses of each mutant to an ~EC_{50} ACh dose before and after exposure to high concentrations of MTSEA (0.5 - 1.0 mM) applied by continuous flow for 30 to 60 seconds. MTSEA was prepared daily in distilled water and stored on ice. Stock solution was diluted to the appropriate working concentration in ESLC immediately before each application. In some cases ($Q^{47}C$, $N^{52}C$), the effect of modification at saturating MTSEA concentrations was accelerated by the presence of ACh. For these mutants, the maximal effect of MTSEA was obtained by co-application of MTSEA and ACh, or by prolonged exposure to MTSEA in the absence of ACh. For mutants which displayed a functional effect of MTSEA, we determined a limiting dose of modifier; oocytes were exposed to low concentrations of MTSEA (0.1-100 μM) for 15-30

Molecular Pharmacology Fast Forward. Published on February 26, 2007 as DOI: 10.1124/mol.106.033092
This article has not been copyedited and formatted. The final version may differ from this version.

seconds, and then challenged with a sub-maximal concentration of ACh. A limiting dose, yielding 20-40% of the maximal MTSEA effect, was identified for each mutant and used to measure modification kinetics. Kinetic data were analyzed as described previously (Pascual and Karlin, 1998).

Structural model of α7 A model of the chick α7 nicotinic receptor extracellular domain, based on the coordinates of the *Lymnea* ACh Binding Protein (Brejc et al., 2001) was constructed as described previously (Lyford et al., 2003; McLaughlin et al., 2006). Images of the model were generated with Pymol (DeLano Scientific, South San Francisco, CA). Distance estimates between amino acids were made using β carbons as a reference point. We estimated the position of the ACh binding using the β carbon of the principal (+) subunit Trp^{148}, the central conserved residue in the aromatic ligand binding pocket (Sine, 2002). We also used a model of the full length human α7 AChR for some of our analysis; coordinates for this model were generously provided by Dr. A. Taly (Université Louis Pasteur, Strasbourg).

Molecular Pharmacology Fast Forward. Published on February 26, 2007 as DOI: 10.1124/mol.106.033092
This article has not been copyedited and formatted. The final version may differ from this version.

Results

A prominent feature of the α7 LBD is a pair of β sheets, the inner and outer sheets, that constitute ~60% of the LBD mass and have been implicated in conformational movements accompanying receptor activation (Brejc et al., 2001; Unwin et. al., 2002). The inner sheet also includes loop 2, the linker sequence between β-strands 1 and 2 that is involved in linkage between the LBD and the TMD (Kash et al., 2003; Chakrapani et al., 2004; Sala et al., 2005; Lee and Sine, 2005). To examine conformational changes in the inner sheet we constructed a series of 18 consecutive single cysteine replacement mutations from L^{36} to I^{53}. This region includes loop 2 and portions of the flanking β1 and β2 strands (Fig. 1). Fourteen of eighteen mutations exhibited acetylcholine-evoked currents when expressed in *Xenopus* oocytes. Four mutants failed to show ACh-evoked currents: a pair of adjacent residues, $Q^{38}C/I^{39}C$, and two leucines, $L^{36}C$ and $L^{49}C$. Of the mutations that expressed functional currents, most had peak currents comparable to the parental phenotype ($C^{115}A/L^{247}T$: EC_{50} 2.3 μM; I_{max} ~ 0.5-5 μA; summarized in Table 1). The exceptions were $D^{41}C$, $N^{46}C$, and $T^{50}C$, which exhibited substantially reduced peak currents (I_{max}~40 nA). Large effects of Cys replacements on ACh-evoked responses were localized to loop 2 ($D^{43}C$ to $Q^{47}C$), a region known to play a role in the gating process (Chakrapani et al., 2004; Lee and Sine, 2005; Kash et al., 2003).

We next examined the susceptibility of the introduced cysteines to chemical modification by measuring dose-responses to ACh before and after exposure to the thiol modifier MTSEA. The goal of these experiments was to identify the cysteines that could be used as reporters for agonist-induced conformational changes. An example of this

Molecular Pharmacology Fast Forward. Published on February 26, 2007 as DOI: 10.1124/mol.106.033092
This article has not been copyedited and formatted. The final version may differ from this version.

analysis, using the $M^{40}C$ mutation as an example, is shown in Fig. 2. Following exposure to MTSEA (10 μM, 30 seconds) the ACh-evoked dose-response curve was shifted to the right and the EC_{50} was increased from 2.3 μM to 36 μM, demonstrating that the introduced thiol group was accessible to the aqueous modifying reagent. When the same MTSEA exposure was done in the presence of a saturating concentration of ACh, however, the shift in dose response curve was substantially smaller (2.3 μM to 11 μM). Thus, the sensitivity of this residue to thiol modification was agonist-dependent, and so can be used to test changes in accessibility or electrostatic environment resulting from ACh-induced conformational changes.

Similar analysis of the entire series of Cys mutants identified 7 additional substitutions that displayed a functional sensitivity to MTSEA (summarized in Table 1). Significant changes in EC_{50} following MTSEA exposure show that of the fourteen receptors that are functionally expressed, at least eight cysteine substitutions in the region between L^{36} and I^{53} have side chains that are accessible to aqueous solvent. Six mutants (plus the $C^{115}A/L^{247}T$ parental phenotype), exhibited no effect of MTSEA application (Table 1); for these we cannot distinguish between a lack of thiol modification and the lack of a functional effect.

Thiol reactivity can be used to explore conformational changes induced by ACh or other ligands. Such conformational sensitivity is best explored by measuring modification rates under resting and activating conditions. Using repeated application of sub-saturating doses of MTSEA it is possible to measure the time- and concentration-dependence of the MTSEA effect. The goal of these modification rate experiments is to

Molecular Pharmacology Fast Forward. Published on February 26, 2007 as DOI: 10.1124/mol.106.033092
This article has not been copyedited and formatted. The final version may differ from this version.

detect ACh-induced changes in side-chain modification accessibility or electrostatic environment. Fig. 3 shows data from one such experiment, using the $E^{44}C$ mutant as an example. Oocytes were challenged with a test dose of ACh (at a concentration near the EC_{50} for that mutant) between brief exposures to a limiting concentration of MTSEA (Fig. 3A). The sequential decrement in currents elicited by the test dose reflected an increasing fraction of receptors that were modified; the endpoint was established with a longer exposure to a high dose of MTSEA. We compared the time course of this current decay with that from another oocyte challenged with the same limiting MTSEA concentration in the presence of saturating ACh (Fig. 3B). In the case of $E^{44}C$ receptors, ACh caused a decrease in the rate of MTSEA modification, suggesting that conformational changes associated with ACh binding drive the $E^{44}C$ side chain to a less accessible position. Normalized data are plotted (Fig. 3C) to extract a rate constant for the reaction between the AChR and the MTSEA (Table 1). These rate constants provide a means to compare the water-accessibility and electrostatic environment of individual residues, as well as the changes in access or environment evoked by ACh binding and activation.

Normalized rate measurements for three additional mutations ($M^{37}C$, $M^{40}C$, and $N^{52}C$) are shown in Figure 4. Based upon models of the α7 LBD the side chains of these three positions should extend toward the subunit-subunit interface in close proximity. Despite this proximity, we observed a qualitative difference in the agonist effect on MTSEA modification; co-application of ACh slowed the rate of modification at $M^{37}C$ and $M^{40}C$ but increased the rate at $N^{52}C$. A plot of the rate constants for MTSEA modification in the absence and presence of saturating concentrations of ACh is shown

Molecular Pharmacology Fast Forward. Published on February 26, 2007 as DOI: 10.1124/mol.106.033092
This article has not been copyedited and formatted. The final version may differ from this version.

in Fig. 5 and the rate constants are provided in Table 1. Overall, four mutants exhibited a decrease in the rate of modification in the presence of ACh; these mutations are either in the β1 strand or in loop 2 ($M^{37}C$, $M^{40}C$, $V^{42}C$, and $E^{44}C$). In general, these mutants exhibited extremely high MTSEA modification rates (5,000-45,000 $M^{-1}s^{-1}$) in the absence of ACh and ~10 fold decreases in modification rates in the presence of ACh. Thus, in the resting conformation these residues were readily accessible to solvent, and were less accessible in the ACh-activated state. At $V^{42}C$, the reaction rate was slow in the absence of ACh (125 $M^{-1}s^{-1}$; ~500 times slower than $E^{44}C$) but also showed a decrease in the presence of ACh, to less than 20 $M^{-1}s^{-1}$.

Modification rates at four other residues were increased in the presence of ACh. At two sites ($Q^{47}C$ and $N^{52}C$) modification rates increased 20- to 40-fold when the MTSEA was co-applied with a saturating dose of ACh. The increase in modification rate in the presence of ACh suggests a movement of these residues from a position of limited accessibility to one of greater accessibility to aqueous solvent. At two additional sites, $D^{43}C$ and $K^{45}C$, we observed a 2- to 3-fold increase in modification rates in the presence of ACh. There is a general trend in which the residues in the β1 strand showed decreased reaction rates during activation whereas residues in the β2 strand showed increased reaction rates. The implications of these agonist-induced changes of side-chain accessibility or environment are discussed below.

Discussion

The inner and outer β sheets comprise the largest structural elements of the LBD of Cys-loop receptors (Brejc et al., 2001). Conformational transitions underlying ligand-

Molecular Pharmacology Fast Forward. Published on February 26, 2007 as DOI: 10.1124/mol.106.033092
This article has not been copyedited and formatted. The final version may differ from this version.

induced activation are likely to involve these structures. In this study we focused on a key region of the inner β sheet: loop 2 and flanking residues in the β1 and β2 strands. By measuring rates of thiol modification we assessed the validity of homology-based models of the α7 AChR extracellular domain. In addition, agonist-induced changes in modification rates provided a test of receptor activation models.

Is the pattern of cysteine modification consistent with structural models?

β1 strand. Structural models (Sine et. al., 2002; Lyford et al., 2003; Taly et al., 2005) predict that M^{37} and M^{40} are on the (-) face of the subunit-subunit interface and accessible to solvent from the outside or from the vestibule of the receptor, respectively. The side-chains of D^{41} and D^{43} are also predicted to be accessible from vestibule of the receptor. Models predict that Q^{38} and I^{39} are buried at the subunit-subunit interface and that V^{42} is buried in the subunit core. The high modification rates of $M^{37}C$ and $M^{40}C$ (5,000-20,000 $M^{-1}s^{-1}$) establish their surface accessibility, in agreement with structural models. We found poor expression and no significant MTSEA effect at $D^{41}C$, providing inconclusive results. There was a small but significant effect of modification at $D^{43}C$, indicating accessibility of this residue, although the modification rate (30 $M^{-1}s^{-1}$) was lower than predicted by the models that show the side-chain projecting toward the vestibule. The modification rate of $V^{42}C$ (125 $M^{-1}s^{-1}$) was also low, suggesting limited accessibility. Overall, our results in the β1 strand suggest that the structural models are valid at most locations, but the data deviate somewhat from the predictions of the models at the C-terminus of β1.

Loop 2. The loop connecting the β1 and β2 strands includes E^{44}, K^{45}, N^{46}, and Q^{47}. The models predict that E^{44}, K^{45}, and Q^{47} are accessible from the outside of the

Molecular Pharmacology Fast Forward. Published on February 26, 2007 as DOI: 10.1124/mol.106.033092
This article has not been copyedited and formatted. The final version may differ from this version.

receptor and that N^{46} is at the subunit-subunit interface and may be accessible from the vestibule. Both $E^{44}C$ and $K^{45}C$ reacted with MTSEA at extremely high rates (>10,000 $M^{-1}s^{-1}$), consistent with a side-chain position that is readily accessible to the aqueous environment. $N^{46}C$ receptors expressed poorly, suggesting that this residue is critical for assembly and/or gating. MTSEA had a small but significant effect on $Q^{47}C$ receptors, also as predicted by models showing this residue to be surface accessible.

The charge at position E^{44} is strongly conserved throughout the Cys-loop family (Fig 1B), and reports have suggested a critical role for this residue in channel gating (Kash et al., 2003; Lee and Sine, 2005). Our result that $E^{44}C$ α7 receptors express at normal levels with an ACh EC_{50} that is elevated only 5-fold above the parental isoform argue against a critical role for E^{44} in the activation of chick α7 AChRs. The high rates of modification we observe at $K^{45}C$ seem inconsistent with a role for this residue in a "pin-and-socket" mechanism (Miyazawa et al., 2003). Similar conclusions were drawn in cysteine accessibility studies of the aligned residue in 5-HT_3 receptors ($K^{81}C$; Reeves et al., 2005). Instead, our results are more consistent with the idea that different members of the Cys-loop receptor family use different molecular interactions during gating (Xiu et al., 2005).

β2 strand. Models predict that the side-chains of V^{48}, T^{50} and N^{52} are accessible to the aqueous environment of the vestibule, whereas those of L^{49}, T^{51}, and I^{53} are buried in the subunit core. Our results were generally consistent with the predictions of the models. $V^{48}C$ and $T^{50}C$ exhibited no functional effect of MTSEA exposure, an inconclusive result because a lack of effect of modification is impossible to distinguish from a lack of MTSEA accessibility. $N^{52}C$ was accessible to MTSEA, as MTSEA greatly

Molecular Pharmacology Fast Forward. Published on February 26, 2007 as DOI: 10.1124/mol.106.033092
This article has not been copyedited and formatted. The final version may differ from this version.

decreased subsequent responses to ACh concentrations up to 3 mM. $L^{49}C$ receptors did not express, suggesting a requirement for a hydrophobic side-chain at this location. Muscle receptors with a leucine-to-lysine substitution at this position also express poorly (Sine et al., 2002). $T^{51}C$ and $I^{53}C$ receptors were insensitive to MTSEA, another inconclusive result but one that is consistent with the structural models.

β1-β2 bend. Three substitutions in β1 and β2, including two adjacent residues ($Q^{38}C$, $I^{39}C$, and $L^{49}C$) yielded receptors that were unresponsive to ACh. Both I^{39} and L^{49} are conserved in Cys-loop receptors (Brejc et al., 2001). In crystal structures of AChBPs (Brejc et al., 2001, Celie et al., 2004; Hansen et al., 2005) and Cys-loop receptor models (Sine et al., 2002; Lyford et al., 2003; Le Novere et al., 2002; Taly et al., 2005) these residues are at a major bend in the β1–β2 strand. The effect of Cys mutations at these positions may indicate the importance of side-chains required to stabilize this structural element.

Are ACh-dependent changes in cysteine modification rates consistent with subunit-rotation models for activation?

Modification rate analysis can be used to measure both the degree of side chain accessibility and changes in accessibility or electrostatic environment during receptor activation. Of the eight Cys replacements where rates of modification were measured, four sites exhibited a protective effect of ACh. At $M^{37}C$, $M^{40}C$, $V^{42}C$, and $E^{44}C$ modification rates decreased 5- to 10-fold in the presence of saturating ACh concentrations. A direct, physical occlusion of modifier accessibility by ACh could explain decreases in modification rate of $M^{37}C$ because of its proximity to the ligand-binding pocket. Physical occlusion, however, is less likely to explain the decreased

Molecular Pharmacology Fast Forward. Published on February 26, 2007 as DOI: 10.1124/mol.106.033092
This article has not been copyedited and formatted. The final version may differ from this version.

reaction rates of $M^{40}C$, $V^{42}C$, or $E^{44}C$ because models suggest that these side-chains are more than 20 Å from the bound ligand. Instead, ACh is likely to cause reduced modification at these sites because of the conformational changes initiated during receptor activation.

We found that ACh caused an increase in modification rates at four positions: $D^{43}C$, $K^{45}C$, $Q^{47}C$, and $N^{52}C$. At these sites, increased rates must be due to conformational changes associated with receptor activation that increase the access of MTSEA to the introduced thiol groups.

The pattern of modification rates and agonist-driven changes in modification rates provide tests of theoretical models for receptor activation. Unwin and colleagues (Miyazawa et al., 2003; Unwin, 2005) propose a model for activation of *Torpedo* AChRs in which ACh binding leads to a clockwise rotation of the LBD and TMD of the two α subunits. Previously we showed that movements around a conserved glutamate in the β8-β9 loop (loop 9) are consistent with rotational models of α7 AChR activation (Lyford et al., 2003).

While the general pattern of ACh effects on modification rates (decreases in β1, increases in β2) might seem compatible with an activation model that involves inner β-sheet rotation, the specific changes in rates we observe at $M^{37}C$, $M^{40}C$, and $N^{52}C$ argue against a simple rotation. In each of these residues, side-chains are exposed to the aqueous cleft on the inner β sheet of the (-) face of the subunit-subunit interface (Fig. 6). The arrangement of the β1 and β2 strands places these side chains in close vertical register, with the N^{52} positioned between M^{37} and M^{40}. If ACh initiates a rotation of the entire β sheet, we expect that the three residues to undergo a concerted movement and

Molecular Pharmacology Fast Forward. Published on February 26, 2007 as DOI: 10.1124/mol.106.033092
This article has not been copyedited and formatted. The final version may differ from this version.

modification rates of all three residues should either increase or decrease. We observed, however, an 8-fold decrease in the modification rates of $M^{37}C$ and $M^{40}C$ but a 25-fold increase in modification rate of $N^{52}C$ (Table 1). It is difficult to reconcile these results with models for ACh activation of nicotinic receptors that that rely on simple rotation of the LBD.

If we presume that the observed changes in modification rates result from multiple conformational perturbations at each site, our results can be brought into line with rotational models. There could be a combination of local (e.g., steric or electrostatic effects of nearby side chains) and global rotational effects that sum to yield a net effect on modification rate. For example, the N^{52} residue is near a conserved Trp residue (W^{54}) that participates in the "aromatic pocket" forming the ACh-binding site (Xie and Cohen, 2001). If ACh binding moves W^{54} away from N^{52}, it could relieve steric or electrostatic constraints and increase MTSEA modification of $N^{52}C$. If, at the same time, the entire inner β sheet rotates to a position of reduced modifier accessibility, the net effect could slow modification rates of other inner β sites such as M^{37} and M^{40} even while modification rate of N^{52} is increased. The difficulty with this idea is magnitude of the rate changes involved. To account for the 25-fold increase in the modification rate of $N^{52}C$, the local effect of W^{54} movement would have to specifically increase N^{52} modification rate 200-fold to overcome the 8-fold decrease in modification caused by the rigid-body rotation.

Molecular Pharmacology Fast Forward. Published on February 26, 2007 as DOI: 10.1124/mol.106.033092
This article has not been copyedited and formatted. The final version may differ from this version.

Conclusions

Overall, our results are consistent with the structural models of α7 nicotinic receptors derived from the structure of AChBPs. Our results, however, are not consistent with models for receptor activation that rely strictly on rigid-body rotation of the LBD. Instead, our results suggest that a combination of local conformational changes, leveraged movements of β-sheets (McLaughlin et al., 2006) that could cause tilting of transmembrane α-helices (Cheng et al., 2006), and rotation of the TMD relative to the LBD (Law et al., 2005) all may be components of the "conformational wave" (Grosman et al., 2001) that transmits information from the ligand-binding site to the gate of the channel.

References

Beene DL, Brandt GS, Zhong W, Zacharias NM, Lester HA, Dougherty DA. (2002) Cation-π interactions in ligand recognition by serotonergic (5-HT_{3A}) and nicotinic acetylcholine receptors: the anomalous binding properties of nicotine. *Biochemistry* **41**: 10262-10269.

Bouzat C, Gumilar F, Spitzmaul G, Wang HL, Rayes D, Hansen SB, Taylor P, Sine SM. (2004) Coupling of agonist binding to channel gating in an ACh-binding protein linked to an ion channel. *Nature*. **430**:896-900.

Brejc K, van Dijk WJ, Klaassen RV, Schuurmans M, van Der Oost J, Smit AB, Sixma TK. (2001) Crystal structure of an ACh-binding protein reveals the ligand-binding domain of nicotinic receptors. *Nature*. **411**:269-76.

Celie PH, van Rossum-Fikkert SE, van Dijk WJ, Brejc K, Smit AB, Sixma TK. (2004) Nicotine and carbamylcholine binding to nicotinic acetylcholine receptors as studied in AChBP crystal structures. *Neuron*. **41**:907-14.

Chakrapani S, Bailey TD, Auerbach A. (2004) Gating dynamics of the acetylcholine receptor extracellular domain. *J Gen Physiol.* **123**:341-56

Cheng X, Wang H, Grant B, Sine SM, McCammon JA. (2006) Targeted Molecular Dynamics Study of C-Loop Closure and Channel Gating in Nicotinic Receptors. *PLoS Comput Biol*. **2**:1173-1184.

Eddins D, Sproul AD, Lyford LK, McLaughlin JT, Rosenberg RL. (2002) Glutamate 172, essential for modulation of $L^{247}T$ alpha7 ACh receptors by Ca^{2+}, lines the extracellular vestibule. *Am J Physiol Cell Physiol*. **283**:C1454-60.

Grosman C, Zhou M, Auerbach A (2000) Mapping the conformational wave of acetylcholine receptor channel gating. *Nature*. **403**:773-6.

Hansen SB, Sulzenbacher G, Huxford T, Marchot P, Taylor P, Bourne Y. (2005) Structures of *Aplysia* AChBP complexes with nicotinic agonists and antagonists reveal distinctive binding interfaces and conformations. *EMBO J*. **24**:3635-3646.

Karlin A. (2002) Emerging structure of the nicotinic acetylcholine receptors. *Nat Rev Neurosci*. **3**:102-14.

Karlin A, Akabas MH. (1998) Substituted-cysteine accessibility method. *Methods Enzymol*. **293**:123-45.

Kash TL, Jenkins A, Kelley JC, Trudell JR, Harrison NL (2003) Coupling of agonist binding to channel gating in the $GABA_A$ receptor. *Nature* **421**:272-275.

Law RJ, Henchman, RH, McCammon JA. (2005) A gating mechanism proposed from a simulation of a human alpha7 nicotinic acetylcholine receptor.
Proc Natl Acad Sci U S A. **102**:6813-8.

Lee WY, Sine SM. Principal pathway coupling agonist binding to channel gating in nicotinic receptors. (2005) *Nature.* **438**:243-7.

Le Novere N, Grutter T, Changeux JP. (2002) Models of the extracellular domain of the nicotinic receptors and of agonist- and Ca^{2+}-binding sites. *Proc Natl Acad Sci U S A.* **99**:3210-5.

Lummis SC, Beene DL, Lee LW, Lester HA, Broadhurst RW, Dougherty DA (2005) Cis-trans isomerization at a proline opens the pore of a neurotransmitter-gated ion channel. *Nature*. **438**:248-52.

Lyford LK, Sproul AD, Eddins D, McLaughlin JT, Rosenberg RL. (2003) Agonist-induced conformational changes in the extracellular domain of alpha 7 nicotinic acetylcholine receptors. *Mol Pharmacol*. **64**:650-8.

McLaughlin JT, Fu J, Sproul AD, Rosenberg RL. (2006) Role of the outer beta-sheet in divalent cation modulation of alpha7 nicotinic receptors. *Mol Pharmacol*. **70**:16-22.

Miyazawa A, Fujiyoshi Y, Unwin N. (2003) Structure and gating mechanism of the acetylcholine receptor pore. *Nature*. **423**:949-55.

Mukhtasimova N, Free C, Sine SM. (2005) Initial coupling of binding to gating mediated by conserved residues in the muscle nicotinic receptor. *J Gen Physiol*. **126**:23-39.

Pascual JM, Karlin, A (1998) State-dependent accessibility and electrostatic potential in the channel of the acetylcholine receptor. Inferences from rates of reaction of thiosulfonates with substituted cysteines in the M2 segment of the alpha subunit. *J Gen Physiol.* **111**:717-39.

Reeves DC, Jansen M, Bali M, Lemster T, Akabas MH (2005) A Role for the β1-β2 loop in the gating of 5-HT3 receptors. *J. Neurosci* **25**:9358-9366.

Revah F, Bertrand D, Galzi JL, Devillers-Thiery A, Mulle C, Hussy N, Bertrand S, Ballivet M, Changeux JP (1991) Mutations in the channel domain alter desensitization of a neuronal nicotinic receptor. *Nature.* **353**:846-9.

Sala F, Mulet J, Sala S, Gerber S, Criado M. (2005) Charged amino acids of the N-terminal domain are involved in coupling binding and gating of α7 nicotinic receptors. *J Biol Chem* **280**: 6642-6647.

Sine SM. (2002) The nicotinic receptor ligand binding domain. *J Neurobiol*. **53**:431-46.

Sine SM, Engel AG. (2006) Recent advances in Cys-loop receptor structure and function. *Nature* **440**: 448-455.

Sine SM, Wang HL, Bren N. (2002) Lysine scanning mutagenesis delineates structural model of the nicotinic receptor ligand binding domain. *J. Biol. Chem*. **277**: 29210-29223.

Taly A, Delarue M, Grutter T, Nilges M, Le Novere N, Corringer PJ, Changeux JP. (2005) Normal mode analysis suggests a quaternary twist model for the nicotinic receptor gating mechanism. *Biophys J*. **88**:3954-65

Unwin N. (2005) Refined structure of the nicotinic acetylcholine receptor at 4A resolution. *J Mol Biol*. **346**:967-89.

Unwin N, Miyazawa A, Li J, Fujiyoshi Y. (2002) Activation of the nicotinic acetylcholine receptor involves a switch in conformation of the alpha subunits. *J Mol Biol*. **319**:1165-1176.

Unwin, N. (1993) Nicotinic acetylcholine receptor at 9 A resolution. *J Mol Biol*. **229**:1101-1124.

Xie Y and Cohen JB (2001) Contributions of *Torpedo* nicotinic acetylcholine receptor gamma Trp-55 and delta Trp-57 to agonist and competitive antagonist function. *J Biol Chem*. **276**:2417-26

Xiu X, Hanek AP, Wang J, Lester HA, Dougherty DA. (2005) A unified view of the role of electrostatic interactions in modulating the gating of cys loop receptors. *J. Biol. Chem*. **280**:41655-41666.

Molecular Pharmacology Fast Forward. Published on February 26, 2007 as DOI: 10.1124/mol.106.033092
This article has not been copyedited and formatted. The final version may differ from this version.

Footnotes

This work was funded by a grant from NIDA (DA 017882) to RLR.

Molecular Pharmacology Fast Forward. Published on February 26, 2007 as DOI: 10.1124/mol.106.033092
This article has not been copyedited and formatted. The final version may differ from this version.

Legends to figures

Figure 1. **Structure and sequence of the chick α7 AChR inner β sheet.**
(A) Model of the extracellular domain. For simplicity, two of the five subunits are omitted. The view is from the inside of the extracellular vestibule. The inner (cyan) and outer (yellow) β sheets, are highlighted in the three subunits shown. The C loops (orange) are located behind the subunits in this view. Residues targeted for SCAM are shown in the center subunit; the lower half of β1 (L^{36} to D^{43}) is green, loop 2 (E^{44}-Q^{47}) is red, and the lower half of β2 (V^{48}-I^{53}) is purple. Note that the loop 2 residues extend into the subunit-subunit interface from the principal binding subunit (left interface of the center subunit) while the β1 and β2 segments line the vestibule and the lower interface of the complementary subunit (right interface). **(B) Sequence alignment of β1-loop2-β2 region of cys-loop receptors.** This region includes 3 residues that are absolutely conserved in all cys-loop receptors (starred positions) and 4 others that show relative conservation, including I^{39} and E^{44}. The portion of β1 that shows the highest degree of conservation (L^{34}-E^{44}) forms part of the subunit-subunit interface in the ACh binding proteins (Brejc et al, 2001). Residues underlined were included in this cysteine scanning study.

Figure 2. Functional effects of MTSEA on $M^{40}C$ α7 AChRs. Open circles: ACh dose-response relationship before exposure to MTSEA (EC_{50} =2.6 μM). Open squares: ACh dose response after a 30-second exposure to 10 μM MTSEA (EC_{50} = 36 μM). Filled squares: ACh dose response (EC_{50} = 11 μM) after a 30-second exposure to 10 μM MTSEA in the presence of 30 μM ACh. Thus, the effect of MTSEA was attenuated in the presence of ACh. Data are normalized from three determinations.

Figure 3. ACh affects the rate of MTSEA modification. (A) ACh-evoked currents (10 μM, open bars) of α7 $E^{44}C$ AChRs were inhibited by repeated exposure to limiting doses of MTSEA (1 μM, 15 sec, grey bars). The maximal effect of MTSEA (0.5 mM, 60 sec, black bars) was measured after four limited exposures. **(B)** ACh-evoked currents

Molecular Pharmacology Fast Forward. Published on February 26, 2007 as DOI: 10.1124/mol.106.033092
This article has not been copyedited and formatted. The final version may differ from this version.

(10 μM, open bars) were less inhibited when repeated limiting MTSEA exposures (1 μM) were in the presence of a saturating ACh concentration (100 μM ACh, grey bars). Current responses elicited by the co-application of MTSEA and ACh are not shown. **(C)** Normalized data of $\{I(t)-I(\infty)\}/\{I(0)-I(\infty)\}$, where I(t) is the current after each exposure to 1 μM MTSEA for cumulative time t, I(0) is the initial current before MTSEA exposure, and I(∞) is the current after the maximal exposure to MTSEA (0.5 mM, 60 sec). Data were obtained in the absence of ACh (filled squares) or in the presence of 100 mM ACh (open squares). Data are fit to a single exponential decay to derive a pseudo first-order rate constant for reaction between the $E^{44}C$ side chain and MTSEA.

Figure 4. ACh decreases the rate of MTSEA modification of $M^{37}C$ and $M^{40}C$, but increases the rate of modification of $N^{52}C$. Data were obtained and plotted as described in Figure 3. The modification rates of each mutant were determined with a limiting dose of MTSEA, indicated in each panel.

Figure 5. ACh alters the MTSEA modification rates of most Cys substitutions in the β1-loop2-β2 region. Modification rates were measured in the absence (squares) or presence (triangles) of saturating ACh concentrations. Downward triangles indicate residues in which the modification rates were *decreased* by ACh ($M^{37}C$, $M^{40}C$, $V^{42}C$, $E^{44}C$). Upward triangles indicate residues in which modification rates were *increased* by ACh ($D^{43}C$, $K^{45}C$, $Q^{47}C$, $N^{52}C$). Rate data from 2-4 separate determinations are averaged.

Figure 6. Alignment of residues M^{37}, M^{40}, and N^{52}. **(A)** Model of α7 LBD viewed from below. As with Fig. 1, two subunits are omitted for simplicity. Each subunit includes an inner (cyan) and an outer (yellow) β sheet. The C-loops form the outer boundary for the two subunit-subunit interfaces shown. Positions of the three residues on the (-) face of the left interface are shown in stick format: M^{37} (green), M^{40} (blue), and N^{52} (purple). **(B)** A view of the (-) face, viewed from across the interface (from the arrow in A). A single monomer is shown with the interface between the LBD and TMD (including loop 2, in red) at the bottom. The atoms of M^{37}, M^{40}, and N^{52} are shown as spheres to emphasize

Molecular Pharmacology Fast Forward. Published on February 26, 2007 as DOI: 10.1124/mol.106.033092
This article has not been copyedited and formatted. The final version may differ from this version.

their proximity. The color scheme for carbon atoms is: M^{37} (green); M^{40} (blue); N^{52}, (purple). Color scheme for other atoms is: nitrogen (dark blue); oxygen (red); sulfur (orange).

mutant	Before MTSEA exposure		MTSEA effect ?	After MTSEA exposure			modification rate, $M^{-1}s^{-1}$	
	ACh EC_{50}, μM	I_{max}, μA		ACh EC_{50}, μM	I_{max}, μA	I_{max}, % control	- ACh (n)	+ ACh (n)
$C^{115}A/L^{247}T$	2.4 ± 0.1	5.0 ± 0.7	-					
$M^{37}C$	2.3 ± 0.3	0.4 ± 0.2	+	>1000*	0.05 ± 0.03*	13*	$4.7\pm1.1 \times 10^3$ (8)	$6.3\pm1.3 \times 10^2$ (5)
$M^{40}C$	2.6 ± 0.4	1.5 ± 0.3	+	22 ± 5.8	1.3 ± 0.4	87	$2.7\pm0.8 \times 10^4$ (6)	$3.2\pm0.8 \times 10^3$ (4)
$D^{41}C$	9.1 ± 2.0	0.04 ± 0.01	-					
$V^{42}C$	7.7 ± 0.4	1.0 ± 0.3	+	46 ± 11	0.7 ± 0.4	70	$1.2\pm0.4 \times 10^2$ (3)	$1.6\pm0.7 \times 10^1$ (2)
$D^{43}C$	46 ± 3.4	0.5 ± 0.1	+	54 ± 4.4	0.5 ± 0.2	100	$3.5\pm0.4 \times 10^1$ (3)	$7.1\pm0.9 \times 10^1$ (2)
$E^{44}C$	12 ± 1.3	5.6 ± 0.7	+	27 ± 1.0	4.9 ± 0.08	88	$6.3\pm2.4 \times 10^4$ (7)	$4.9\pm1.1 \times 10^3$ (4)
$K^{45}C$	71 ± 22	3.5 ± 0.2	+	45 ± 7.3	3.5 ± 0.4	100	$2.1\pm5.3 \times 10^4$ (5)	$5.9\pm1.1 \times 10^4$ (4)
$N^{46}C$	15 ± 0.6	0.04 ± 0.01	-					
$Q^{47}C$	60 ± 11	1.5 ± 0.1	+	39 ± 7.6	1.2 ± 0.1	80	$2.5\pm1.2 \times 10^1$ (5)	$1.0\pm0.2 \times 10^3$ (6)
$V^{48}C$	11 ± 2.1	4.1 ± 0.9	-					
$T^{50}C$	9.3 ± 0.4	0.03 ± 0.01	-					
$T^{51}C$	4.3 ± 0.3	1.3 ± 0.5	-					
$N^{52}C$	13 ± 3.0	0.4 ± 0.2	+	>1000*	0.02 ± 0.01*	5*	$6.8\pm3.5 \times 10^1$ (4)	$1.7\pm0.3 \times 10^3$ (3)
$I^{53}C$	1.6 ± 0.1	5.1 ± 0.6	-					

Table 1. Properties of α7 AChR Cysteine Mutants of the β1-loop2-β2 region. The EC_{50} and I_{max} measurements for each receptor mutation represent mean values (± SEM) from at least 3 separate experiments. For dose-response relationships that did not reach a plateau (indicated by *), EC_{50} and I_{max} values represent a lower limit. Mutants that had an MTSEA effect (indicated by +) had a statistically significant different EC_{50} after MTSEA exposure (paired t-test, $p<0.05$).

Molecular Pharmacology Fast Forward. Published on February 26, 2007 as DOI: 10.1124/mol.106.033092
This article has not been copyedited and formatted. The final version may differ from this version.

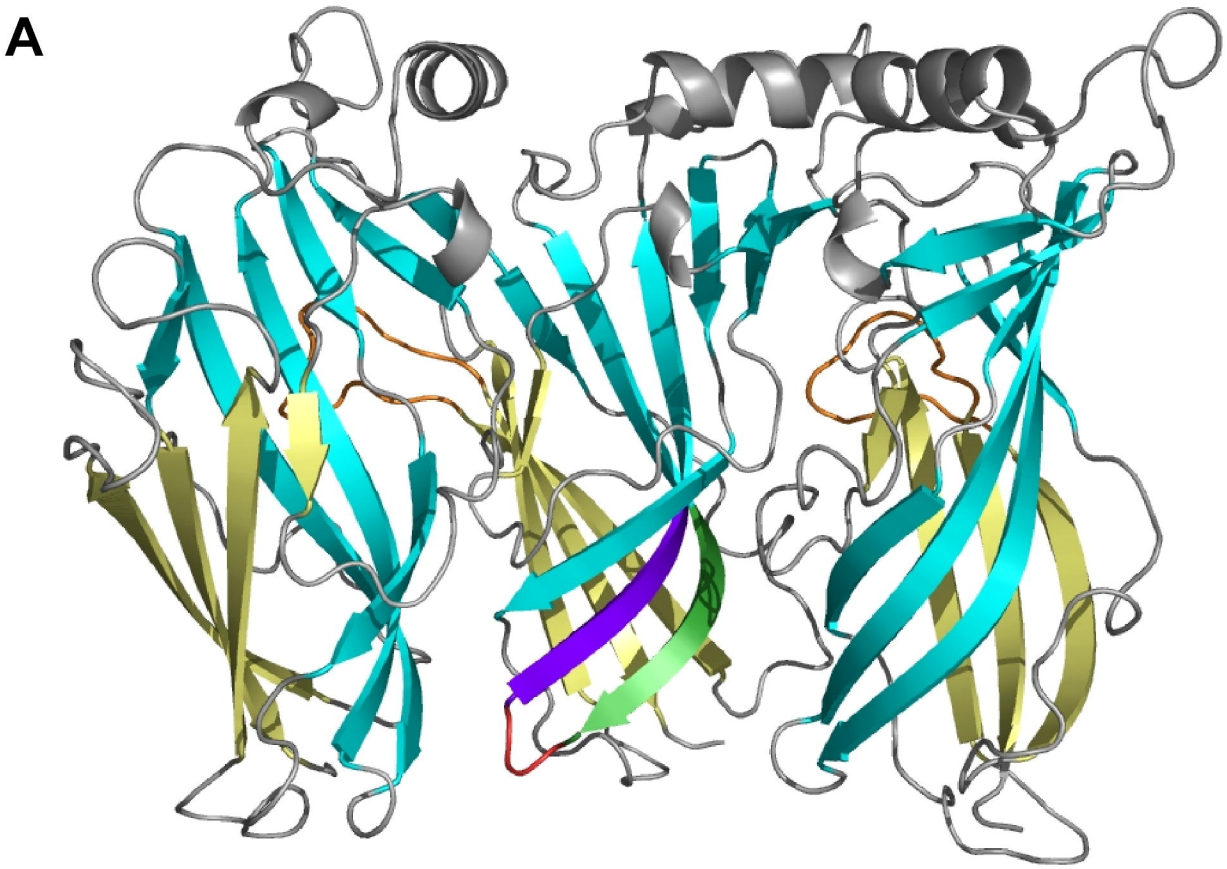

Figure 1

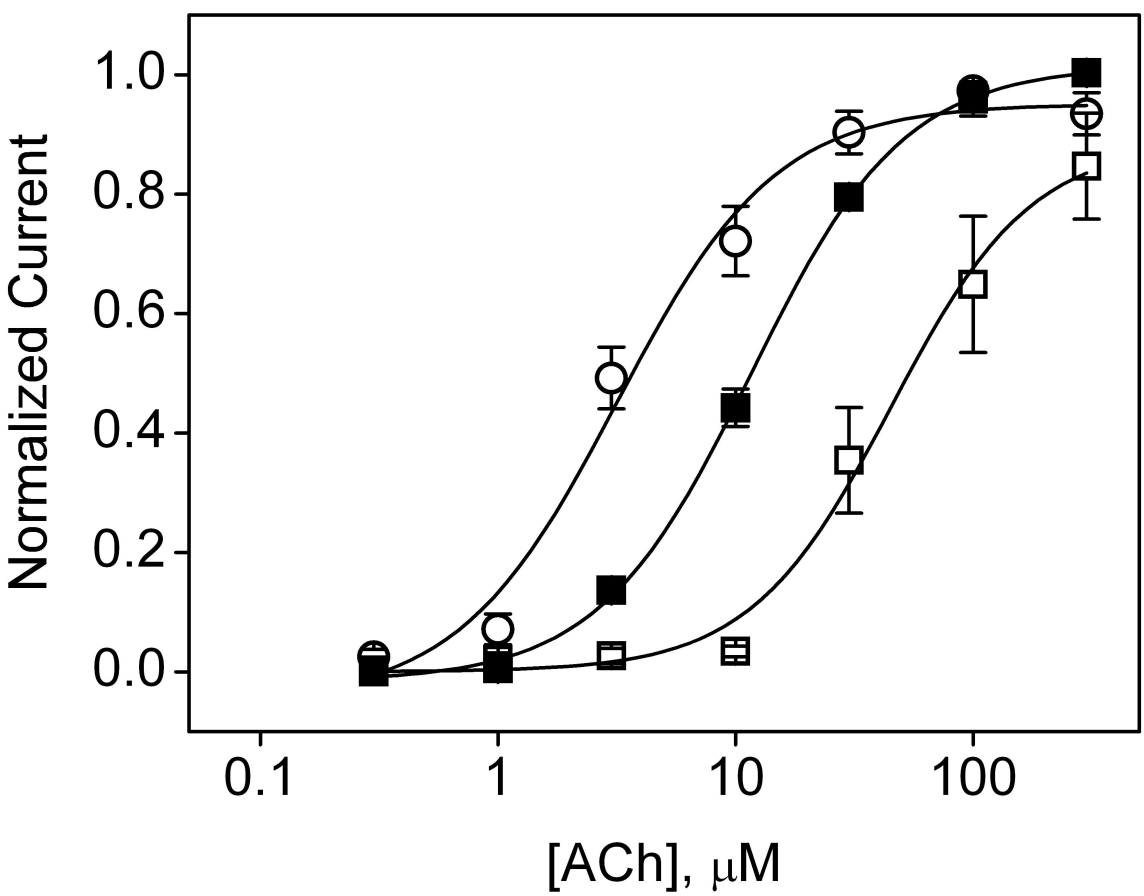

Figure 2

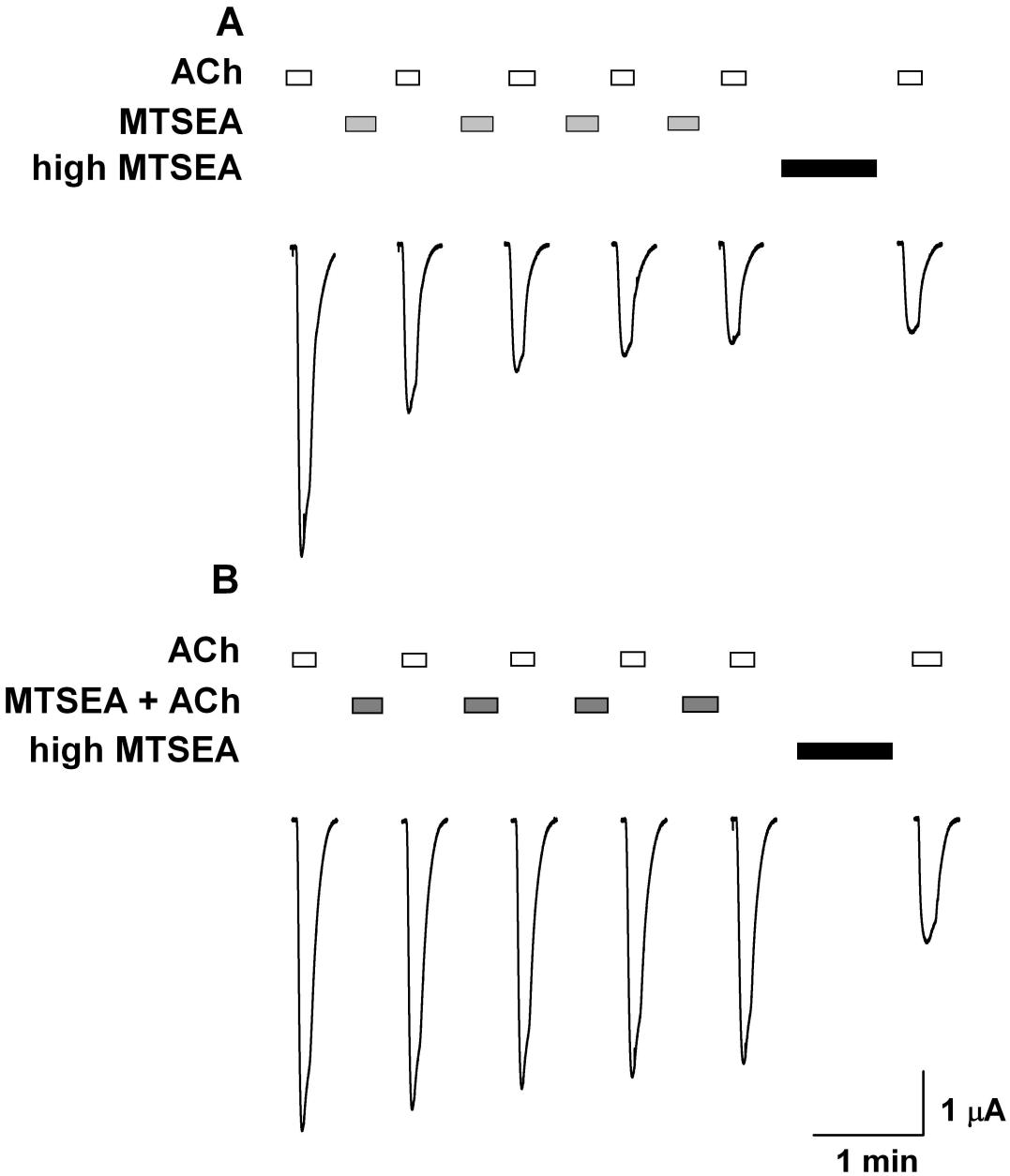
A
ACh
MTSEA
high MTSEA
B
ACh
MTSEA + ACh
high MTSEA
1 μA
1 min
C
Normalized [I-I infinity]
1.0
0.8
0.6
0.4
0.2
0.0
+ACh
-ACh
0
20
40
60
MTSEA exposure, seconds

Figure 3

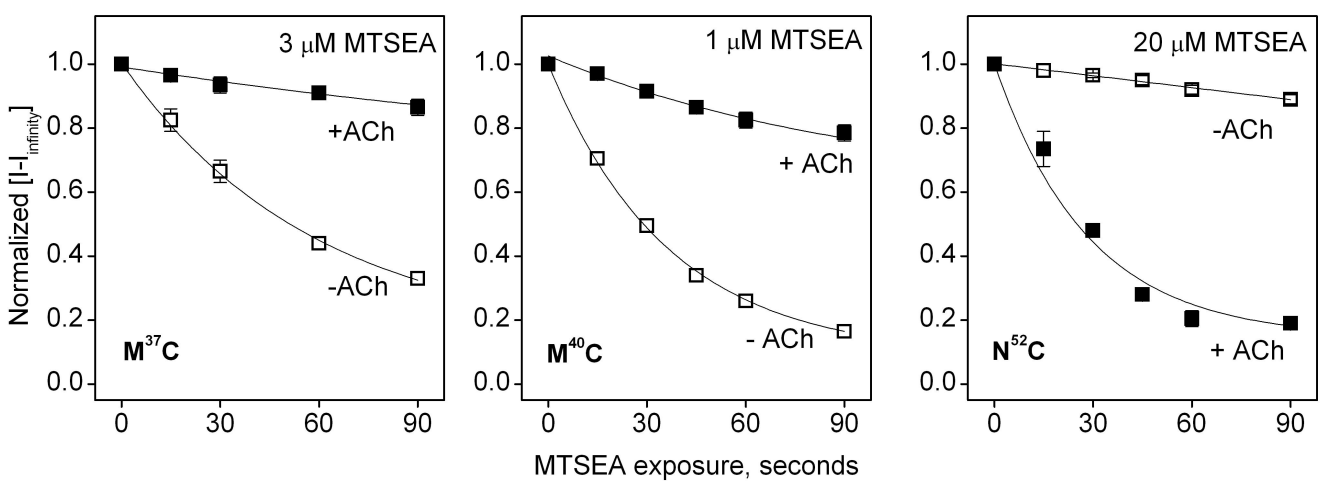
3 μM MTSEA
+ACh
-ACh
M37C
1 μM MTSEA
+ ACh
- ACh
M40C
20 μM MTSEA
-ACh
+ ACh
N52C
Normalized [I-I infinity]
MTSEA exposure, seconds
0.0
0.2
0.4
0.6
0.8
1.0
0
30
60
90

Figure 4

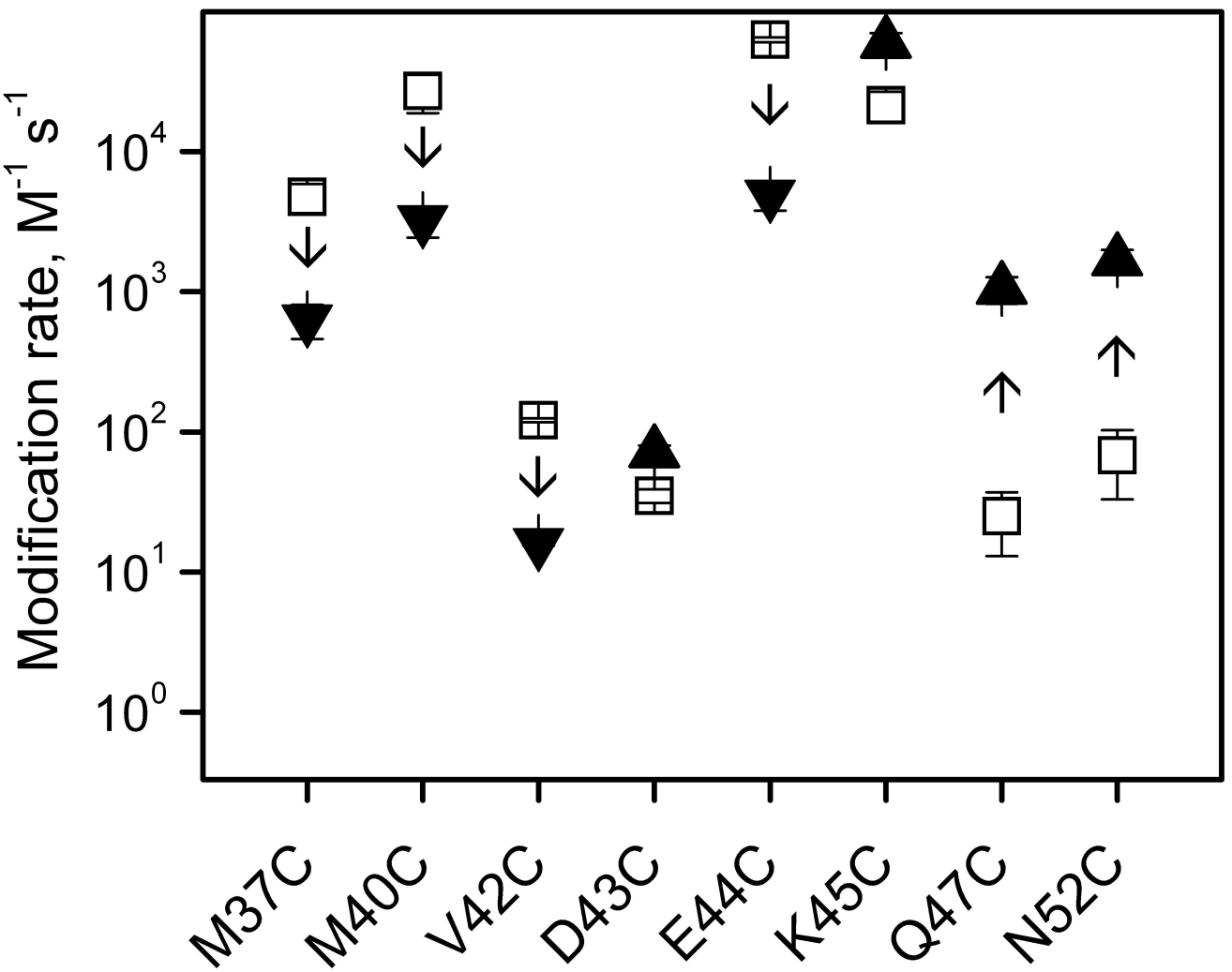
Modification rate, M-1 s-1
10^4
10^3
10^2
10^1
10^0
M37C
M40C
V42C
D43C
E44C
K45C
Q47C
N52C

Figure 5

Molecular Pharmacology Fast Forward. Published on February 26, 2007 as DOI: 10.1124/mol.106.033092
This article has not been copyedited and formatted. The final version may differ from this version.

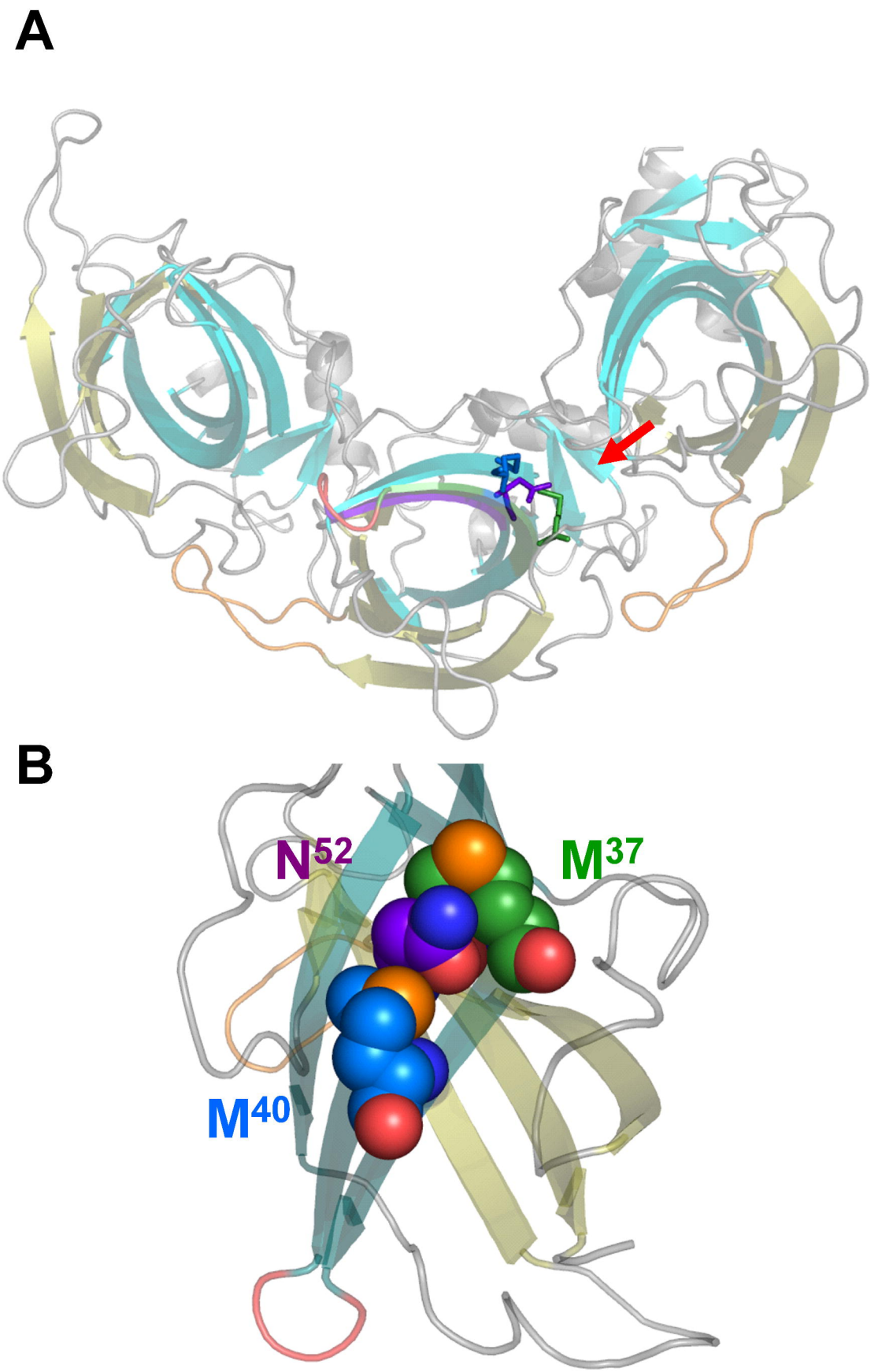

Figure 6